# Transorbital Approaches to the Middle Fossa: Morphometric Analysis and Anatomical Relevance.

Luis Carlos Avellaneda[1,6], María Juliana Arteaga[1], Wilmer Ruiz[1], Dharma Arias[1,3], Nicolás Granados[1,2], Sarita Aristizabal Ortiz[1,6], Diana Bel Rivas Caicedo[5],Lorena Garcia Agudelo[4], Jorge Humberto Aristizabal[6], Edgar Ordoñez Rubiano[1,7]

*1.Department of Neurosurgery, Hospital Universitario Fundación Santa Fé de Bogotá, 2.School Of Medicine, Universidad de los Andes, 3.School Of Medicine, Universidad del Norte, 4.Research department Gihoro, Hospital Regional de Orinoquía, 5.National Institute of Forensic Medicine, Bogotá, 6.Neurosurgery Residency Program, Universidad el Bosque. 7. Hospital de San José, Fundación Universitaria de Ciencias de la Salud, Bogotá, Colombia*

## Introduction

Over the past decade, the endoscopic transorbital approach (eTOA) has become established as a minimally invasive alternative to traditional transcranial and endonasal approaches for the treatment of skull base lesions. This approach provides direct access to the middle cranial fossa, the sphenoid wing, and Meckel's cave, with reduced brain retraction and a lower risk of injury to critical neurovascular structures. However, the morphometric parameters described for surgical planning are derived mainly from studies conducted in European and Asian populations, which limits their extrapolation to other settings due to potential anthropometric differences.

In Latin America, and particularly in Colombia, there are no studies that systematically document these anatomical characteristics in the context of transorbital approaches. Accordingly, the aim of the present study is to describe the anatomical dimensions relevant to transorbital access to the middle and anterior cranial fossae in the Colombian population, in order to optimize surgical planning, reduce intraoperative risks, and provide comparative data with international relevance for the advancement of skull base surgery in the region.

## Methods and Materials

A descriptive observational study was conducted on adult cadaveric over 18 years of age. These specimens underwent forensic necropsy at the National Institute of Forensic Medicine – Bogotá Office. Thirty-one heads were analyzed, with 62 measurements performed using ETOA.

Multiple measurements of orbital structures and the medial cranial fossa were taken. such as height, width, depth to the superior orbital fissure (SOF), working window, bone wall thickness, distance to the rotundum, oval foramen, and trigeminal ganglion. The objective was to analyze distance averages and possible bilateral differences. For comparisons between the two sides, the student t test for related samples was used, considering a significance level of $p < 0.05$. Additionally, working angles were measured in the vertical and horizontal planes to compare the different windows (1: <10x10, 2:10x10 – 12x12, 3: >12x12) (Figure 1) and their angles using the nonparametric Kruskal-Wallis test. (Figure 2). Statistical analysis was performed using SPSS software.

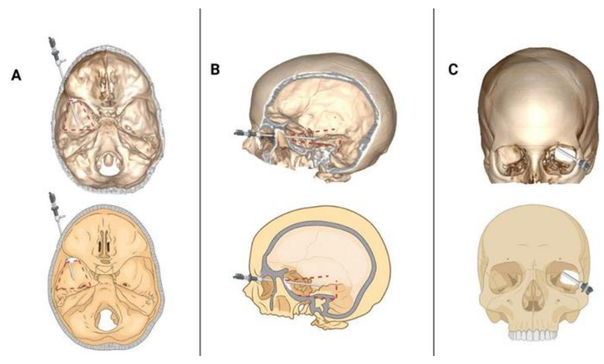


**Figure 1.** **Endoscopic transorbital approach to the skull base.**
(A) Axial superior view showing the extradural surgical corridor.
(B) Lateral reconstruction illustrating the transorbital trajectory.
(C) Anterior view showing the orbital entry point and instrument orientation.

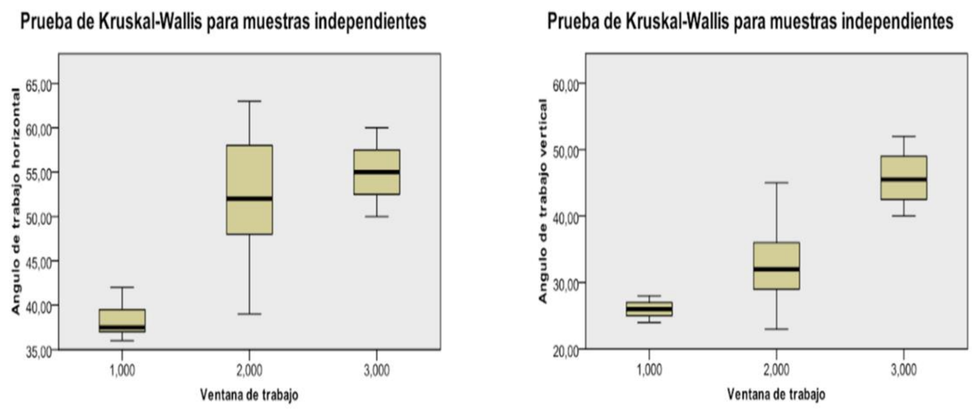


**Figure 2.** Comparison of working window horizontal and vertical vs workingangle.

## Results

The orbital width, height, depth, and bone thickness were assessed. The average width was 41.4 mm (35–50 mm) with moderate variability and no significant differences between sides ($p = 0.4758$). The average height was 29.9 mm (25–35 mm) with low dispersion and bilateral symmetry ($p = 0.4436$). Orbital depth averaged 42.35 mm (33–50 mm), also with no differences between sides ($p = 0.3749$). Bone thickness showed greater variability, averaging 6.9 mm (4–13 mm), although not statistically significant ($p = 0.2845$). (Table 1)

## Results

The mean distance to the rotundum, and ovale foramen was 54.4 mm, and 65.91 mm respectively, to the Gasserian ganglion 70.93 mm. There were no significant differences between sides ($p > 0.05$), indicating bilateral anatomical symmetry. The mean working angle was 50.21° horizontally and 32.38° vertically. (Table 1)

When evaluating the relationship between the size of the working window and the horizontal angle, Window 1 showed the smallest and most consistent angles, with values around 38°, reflecting a significant limitation in the range of motion. In contrast, Windows 2 and 3 showed considerably larger angles, with medians close to 52° and 55°, respectively. Meanwhile, the vertical working window showed working angles between 26°, 31°, and 45° for Windows 1, 2, and 3, respectively. (Table 1)

| *Orbit measurements* | *Average* | *Minimum* | *Maximum* | *SD* | *CI 95%* | *p- value* |
|---|---|---|---|---|---|---|
| Orbit width measurement (mm) (n = 62) | 41,4 | 35 | 50 | 4,13 | | |
| Measurement of orbital width (mm) RE (n = 31) | 41,45 | | | 4,14 | (39,99-42,91) | 0,4758 |
| Measurement of orbital width (mm) LE (n = 31) | 41,39 | | | 4,21 | (39,91-42,87) | |
| Measurement of the height of the orbit (mm) (n= 62) | 29,9 | 25 | 35 | 2,65 | | |
| Orbital height measurement (mm) RE (n = 31) | 29,94 | | | 2,71 | (28,98-30,89) | 0,4436 |
| Measurement of the upper orbit (mm) LE (n = 31) | 30,03 | | | 2,64 | (29,10-30,96) | |
| Measurement of orbital depth (mm) (from the superolateral end to the SOF) (n=62) | 42,35 | 33 | 50 | 4,72 | | |
| Measurement of orbital depth (mm) RE (n = 31) | 42,16 | | | 4,75 | (40,49-43-84) | 0,3749 |
| Measurement of orbital depth (mm) LE (n = 31) | 42,55 | | | 4,76 | (40,87-44,22) | |
| Bone wall thickness (mm) (n=62) | 6,9 | 4 | 13 | 2,64 | | |
| Bone wall thickness (mm) RE (n = 31) | 6,71 | | | 2,45 | (5,85-7,57) | 0,2845 |
| Bone wall thickness (mm) LE (n = 31) | 7,1 | | | 2,86 | (6,09-8,10) | |
| ***Measurements of the middle cranial fossa*** | | | | | | |
| Distance to the round foramen (mm) (from the supero-lateral end) (n=62) | 54,4 | 42 | 61 | 4,45 | | |
| Distance to round foramen (mm) RE (n=31) | 54,58 | | | 4,64 | (52,95-56,21) | 0,3784 |
| Distance to round foramen (mm) LE (n=31) | 54,23 | | | 4,33 | (52,70-55,75) | |
| Distance to foramen ovale (mm) (from the supero-lateral end) (n=62) | 65,91 | 57 | 74 | 4,23 | | |
| Distance to foramen ovale (mm) RE (n=31) | 65,97 | | | 4,15 | (64,51-67,43) | 0,4646 |
| Distance to foramen ovale (mm) LE (n=31) | 65,87 | | | 4,38 | (64,33-67,41) | |
| Distance to the gasserian ganglion (mm) (from the supero-lateral end) (n=62) | 70,93 | 62 | 78 | 3,92 | | |
| Distance to the gasserian ganglion (mm) RE (n=31) | 70,84 | | | 3,86 | (69,48-72,20) | 0,424 |
| Distance to the gasserian ganglion (mm) LE (n=31) | 71,03 | | | 4,05 | (69,61-72,46) | |
| Middle fossa horizontal working angle (Degrees) (n=62) | 50,21 | 36 | 63 | 7,88 | | |
| Middle fossa horizontal working angle RE (n=31) | 50,74 | | | 11,46 | (46,71-54,78) | 0,3577 |
| Middle fossa horizontal working angle LE (n=31) | 49,68 | | | 11,41 | (45,66-53,69) | |
| Middle fossa vertical working angle (Degrees) (n=62) | 32,38 | 23 | 52 | 6,22 | | |
| Middle fossa vertical working angle RE (n=31) | 33 | | | 9,26 | (29,74-36,26) | 0,2880 |
| Middle fossa vertical working angle LE (n=31) | 31,77 | | | 7,85 | (29,01-34,54) | |

**Table 1.** Statistical analysis by variables

## Discussion

This study provides original morphometric data on the endoscopic transorbital approach (eTOA) to the middle cranial fossae in a Colombian population, establishing a local anatomical reference for skull base surgical planning. Compared with European and Asian series, greater distances to deep anatomical structures and significantly wider horizontal and vertical working angles were observed, suggesting potentially larger surgical corridors, likely related to population-specific craniofacial variations. These findings highlight the importance of incorporating population-based anatomical parameters to optimize safety and efficacy, minimize the risk to critical neurovascular structures, and support the need to tailor eTOA planning to regional morphometric characteristics.

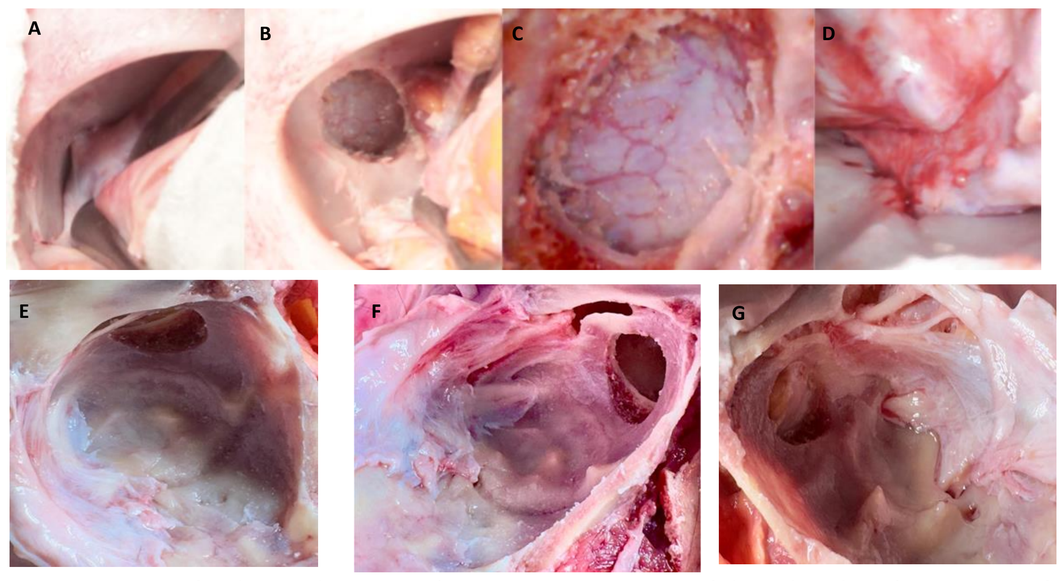


**Figure 3.** Images of cadaveric dissection: A) Anterior-posterior view of the right orbit. B) Osteotomy of the sphenoid bone. C) Working window and exposure of the dura mater. E) Superior view of the right middle cranial fossa. F-G) Superior-lateral view of the right and left middle cranial fossae, respectively.

## Conclusions

Anatomical bilateral symmetry was evident in orbital dimensions, distances to critical structures, and working angles, with no significant differences between sides. The variability in bone thickness highlights the importance of individualized surgical planning to reduce risks during the intervention. Furthermore, there is a significant relationship between surgical window size and working angles, primarily in the horizontal plane. Small windows (<10x10 mm) significantly restrict mobility and the visual field, potentially increasing surgical difficulty and risk. These findings serve as an anatomical reference for optimizing MIS and comparing them with other populations.

## Contact

**Edgar G. Ordoñez-Rubiano, MD**
Fundación Santa Fe de Bogotá
+573006439837
egordonez@fucsalud.edu.co

## References

1. Corvino S, de Notaris M, Sommer D, Kassam A, Kong D-S, Piazza A, et al. Assessing the feasibility of selective piezoelectric osteotomy in transorbital approach to the middle cranial fossa: anatomical and quantitative study and surgical implications. World Neurosurg. 2024;192:e198–e209. doi:10.1016/j.wneu.2024.09.066.
2. Lin B-J, Ju D-T, Hsu T-H, Chung T-T, Liu W-H, Hueng D-Y, et al. Endoscopic transorbital approach to anterolateral skull base through inferior orbital fissure: a cadaveric study. Acta Neurochir (Wien). 2019;161(10):2033–43. doi:10.1007/s00701-019-03993-3.
3. Guizzardi G, Mosteiro A, Hoyos J, Ferres A, Topczewski T, Reyes L, et al. Endoscopic transorbital approach to the middle fossa: qualitative and quantitative anatomic study. Oper Neurosurg. 2022;23(4):E267–E275. doi:10.1227/ons.0000000000000308.
4. Serioli S, Nizzola M, Plou P, De Bonis A, Meyer J, Leonel LCPC, et al. Surgical anatomy of the microscopic and endoscopic transorbital approach to the middle fossa and cavernous sinus: anatomo-radiological study with clinical applications. Cancers (Basel). 2023;15(18):4435. doi:10.3390/cancers15184435.
5. Komaitis S, Skandalakis GP, Drosos E, Neromyliotis E, Charalampopoulou E, Anastasopoulos L, et al. The lateral retrocanthal transorbital endoscopic approach to the middle fossa: cadaveric stepwise approach and review of quantitative cadaveric data. Neurosurg Focus. 2024;56(4):E6. doi:10.3171/2024.1.FOCUS23839.
6. Corvino S, Kassam A, Piazza A, Corrivetti F, Spiriev T, Colamaria A, et al. Open-door extended endoscopic transorbital technique to the paramedian anterior and middle cranial fossae: technical notes, anatomomorphometric quantitative analysis, and illustrative case. Neurosurg Focus. 2024;56(4):E7. doi:10.3171/2024.1.FOCUS23838.
7. Chibbaro S, Ganau M, Scibilia A, Todeschi J, Zaed I, Bozzi MT, et al. Endoscopic transorbital approaches to anterior and middle cranial fossa: exploring the potentialities of a modified lateral retrocanthal approach. World Neurosurg. 2021;150:e74–e80. doi:10.1016/j.wneu.2021.02.095.
8. Houlihan LM, Loymak T, Abramov I, Jubran JH, Knoll AJS, Howshar JT, et al. The biportal transorbital approach: quantitative comparison of the anterior subfrontal craniotomy, bilateral transorbital endoscopic, and microscopic approaches. J Neurosurg. 2024;140(1):59–68. doi:10.3171/2023.4.JNS221866.
9. Park HH, Roh TH, Choi S, Yoo J, Kim WH, Jung IH, et al. Endoscopic transorbital approach to mesial temporal lobe for intra-axial lesions: cadaveric study and case series (SevEN-008). Oper Neurosurg. 2021;21(6):E506–E515. doi:10.1093/ons/opab319.
10. Patel NR, Singhal S, Dhupar V, Kaur M, Agrawal A. Morphometric analysis of the superior orbital fissure in dry adult skulls and its clinical implications. Surg Radiol Anat. 2021;43(8):1335–42. doi:10.1007/s00276-021-02726-3.
Pirinc E, Yilmaz E, Ozturk A, Dagistan Y. Morphometric evaluation of the superior orbital fissure and its symmetry using computed tomography. J Craniofac Surg. 2023;34(3):851–5. doi:10.1097/SCS.0000000000008963.
11. Arslan M, Keles P, Yildiz S, Govsa F. Morphometric analysis of the foramen ovale and trigeminal ganglion: bilateral variations in human cadavers. Anat Sci Int. 2012;87(4):187–95. doi:10.1007/s12565-011-0127-9.